ELSEVIER

Ceramics International 25 (1999) 245–252

CERAMICS INTERNATIONAL

Elongated mullite crystals obtained from high temperature transformation of sillimanite

A. Tomba [a], M.A. Camerucci [a], G. Urretavizcaya [a], A.L. Cavalieri [a], M.A. Sainz [b,*], A. Caballero [b]

[a] *INTEMA, CONICET/UNMdP, Mar de Plata, Argentina*
[b] *Instituto de Cerámica y Vidrio, CSIC, Arganda del Rey, Madrid, Spain*

Received 26 November 1997; accepted 9 February 1998

Abstract

The high temperature transformation of sillimanite to mullite has been studied by means of dilatometry, X-ray diffraction, FT-IR and scanning electron microscopy (SEM-EDS) techniques. The results obtained showed that total transformation of sillimanite to mullite takes place between 1550 and 1600°C. A rapid nucleation occurs above 1550°C due to the resemblance of sillimanite and mullite structures. As a consequence of the high temperature of mullitization of sillimanite, the grain growth of elongated mullite crystals takes place almost simultaneously with the nucleation stage. Finally, a step of acid leaching was employed to remove the glassy phase and high-grade purity mullite powders were obtained.

Keywords: A. Firing; D. Silicate; D. Mullite; Elongated crystals

1. Introduction

Sillimanite, andalusite and kyanite comprise the anhydrous aluminum silicate polymorphs commonly known as the sillimanite group minerals. Such minerals have the same composition ($Al_2O_3.SiO_2$) and transform into mullite and silica at temperatures between 1300 and 1600°C depending on the polymorphic form [1–3]. These raw materials are predominantly consumed within the refractory industry because of their ability to form a mullite phase at high temperatures. This phase confers a high hot strength with good resistance to chemical corrosion and physical erosion.

Mullite-based materials are also an attractive advanced ceramic material because of their optical, dielectric and structural applications. Consequently, several topics related to this material have been studied; phase equilibria, crystalline and amorphous structures, methods of synthesis, thermal evolution of the precursor, densification behaviour and properties [4,5].

The aim of this paper is to study mullite formation by high temperature transformation of sillimanite and to apply a low cost method of purification, based on a leaching step, to remove the glassy phase formed during the transformation and to obtain high-grade purity mullite powders.

2. Experimental procedure

2.1. Raw material

A natural sillimanite from Tacuil (Salta, Argentine [6]) was used as the raw material. After grinding, the fraction higher than 105 mm (S_o) was used to obtain a beneficiated material (S_b). In this step, clays and quartz were eliminated by flotation with amine acetate (pH: 2.5–3.00) and further treatment with bromoform. Biotite and iron compounds were eliminated by magnetic separation.

2.2. Thermal treatments

Sillimanite beneficiated mineral (S_b) was cold isopressed at 200 MPa into cylindrical bars (6 mm in diameter 50 mm in length) and then fired in air between 1500 and 1650°C for 4 h, using a constant heating rate of 5°C/min, in a furnace with molybdenum silicide heating elements. The samples were brought to the

* Corresponding author.

0272-8842/99/$—see front matter
PII: S0272-8842(98)00031-5

required temperature and cooled to room temperature after an appropriate annealing. The samples were polished to 1 μm following which the microstructures of chemically and thermally etched specimens were studied by reflected light optical microscopy (RLOM) and scanning electron microscopy (SEM-EDS).

2.3. Leaching method

The mullitized material selected (1575°C, 4 h) was crushed in a tungsten carbide mortar, milled in an alumina ball mill with balls/solid/water ratio of 2/1/1 and finally, attrition milled using mullite balls of 2–3 mm in diameter and grinding media/solid mass ratio equal to 117/25, in aqueous medium.

The material was leached with 20 ml of 10% HF per gram in a magnetic stirrer at room temperature. After 30 min, the suspension was centrifugated at 3000 rpm, resuspended in hot 50% HCl and centrifugated again. The residue was washed with distilled water until the water residue mixture remained at neutral pH. Finally, the dry powder was precisely weighed to calculate the yield.

2.4. Materials characterization

The chemical compositions were determined by sequential inductively coupled atomic plasma emission spectroscopy (SiO_2, Al_2O_3, Fe_2O_3, TiO_2, CaO, MgO) and flame photometry (Na_2O, K_2O).

The specific surface areas of both samples were determined with a Monosorb Quantachrome meter by the standard BET method, which makes use of the nitrogen adsorption/desorption isotherm.

The real densities of the powders were measured by picnometry in kerosene. The densification degree of the thermally treated materials was analyzed from density measurements by the Archimedes method in distilled water.

The X-ray diffractometric analyses were made using a conventional Siemens D5000 equipment operating at 50 kV and 30 mA, with CuKα radiation.

The FT-IR studies (1400 to 400 cm^{-1}) were carried out in a Perkin Elmer 1760X spectrometer using KBr pelletised samples. DTA/TGA analyses were performed in a Mettler M51 equipment at 10°C/min heating rate up to 1500°C and the dilatometric curves (Adamel Lhomargy) were recorded at a constant heating rate of 10°C/min up to 1600°C, in air.

3. Results and discussion

3.1. Sillimanite characterization

The chemical analyses of the two samples, S_b and S_o, are reported in Table 1. As can be observed, the total impurity content decreased notably in the beneficiated sample, but relatively high amounts of iron and potassium oxide remain in the sample. The iron oxide was detected mainly in solid solution in sillimanite while potassium oxide was associated with the presence of residual muscovite in the beneficiated sample.

The specific surface area value for the beneficiated sample was 0.76 and 2.0 m^2/g for the starting mineral, S_o. This diminution can be assigned to the loss of the fine particle fraction in the beneficiation step.

The real densities of the powders were, $S_o = 3.00\ g/cm^3$ and $S_b = 3.20\ g/cm^3$, which suggest a large contribution of sillimanite ($\rho_{th} = 3.25\ g/cm^3$) in the beneficiated sample.

The XRD patterns corresponding to the starting and beneficiated minerals are shown in Fig. 1; sillimanite, muscovite and quartz were identified in S_o. The main phase in S_b was sillimanite with a limited amount of quartz and traces of muscovite. Both materials were analysed by SEM/EDS. In the starting material (Fig. 2a) large crystals of muscovite and sillimanite with small ones of clays and fine mineral from the initial milling were identified. However, mainly elongated crystals together with limited small crystals of sillimanite were observed in S_b sample (Fig. 2b).

3.2. DTA-TG and dilatometric studies

The DTA-TG analysis (Fig. 3) confirmed the presence of very small amounts of muscovite in the beneficiated sample. At temperatures higher than 800°C, a small endothermic peak in the DTA curve, associated with weight loss in the TG, was detected. This effect was clearly attributed to the loss of structural water of the small amounts of muscovite present in the sample. The value of weight loss determined by thermogravimetric analysis (TG) was 0.76%, in good agreement with the date obtained by chemical analysis (Table 1).

The thermal shrinkage (dL/L_o) of the beneficiated sample was studied as a function of temperature by

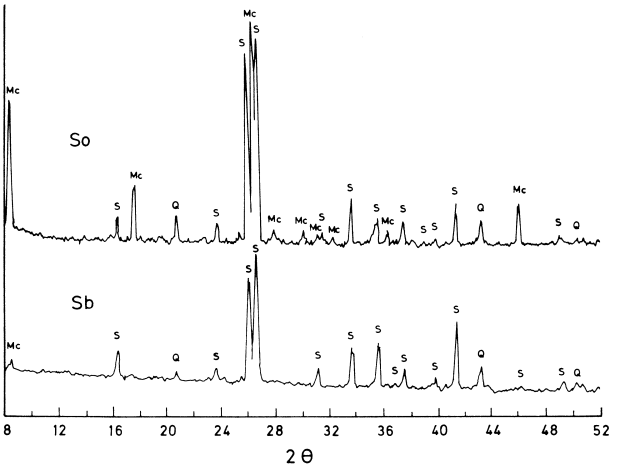

Fig. 1. XRD of original (S_o) and beneficiated (S_b) sillimanite.

dilatometry. In Fig. 4 the various stages of transformation which take place in the sample are shown. At temperatures of approximately 800°C an effect associated with the weight loss from muscovite was scarcely observed. From this temperature up to 950°C the sample clearly showed a limited expansion behaviour, which can be explained by the formation of small amounts of mullite, undetectable by XRD, from minor impurities present in the sample.

From 950°C to approximately 1350°C a contraction effect is observed as consequence of the sintering of the sample in presence of a liquid phase. The presence of liquid phase can be justified by the relatively high level (0.94 wt%) of alkaline oxides present in the sample. An analysis of the ternary system Al_2O_3–SiO_2–K_2O shows that the temperature of first liquid formation takes place at 983°C. So, from this temperature the presence of a liquid phase affects the sample.

At temperatures higher than 1350°C a slight change in the slope of the curve was detected, which can be attributed to the beginning of the sillimanite–mullite transformation. Finally at temperatures between 1550 and 1650°C, where a noticeable increase of the shrinkage rate was observed, took place the larger part of sillimanite–mullite transformation occurred. These interpretations are confirmed by XRD and SEM-EDS studies.

It is important to point out that the dilatometric study does not show the small expansion effect associated with the mullite formation and cristobalite nucleation. On the contrary, an important increase in the shrinkage rate of contraction was detected at very high temperature. These facts can be explained by the presence of the previously mentioned liquid phase formed in the material due to the alkaline impurities. These oxides, $K_2O + Na_2O$, lower the formation

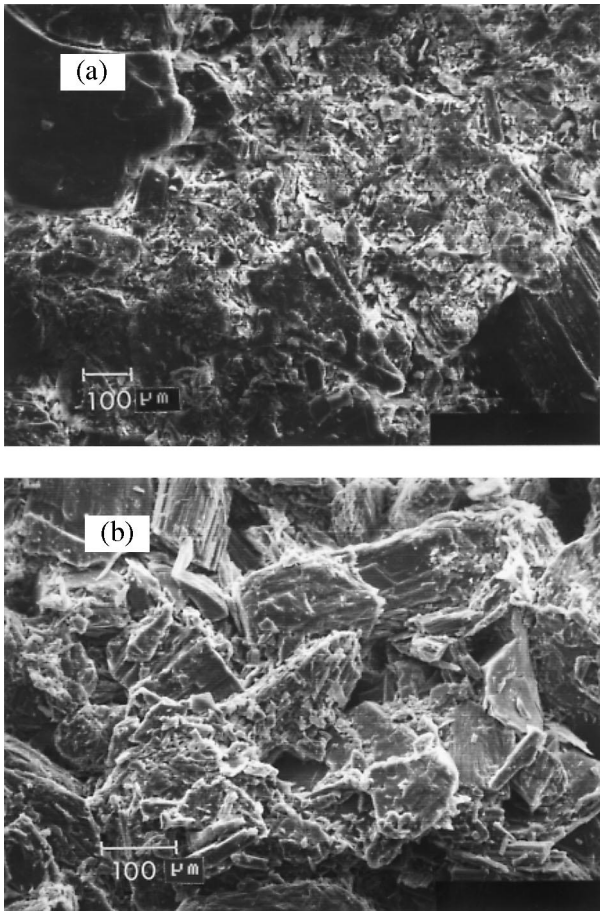

Fig. 2. Scanning electron micrograph showing characteristic of sillimanite minerals. (a) Original (S_o) and (b) beneficiated (S_b) sillimanite.

Table 1
Chemical composition of the sillimanite samples (wt%)

Measured values	S_o	S_b
W.L.	1.93	0.70
SiO_2	45.35	42.15
Al_2O_3	46.09	54.95
Fe_2O_3	1.87	0.76
TiO_2	0.20	0.06
CaO	0.25	0.12
MgO	0.80	0.32
Na_2O	0.41	0.12
K_2O	3.10	0.82

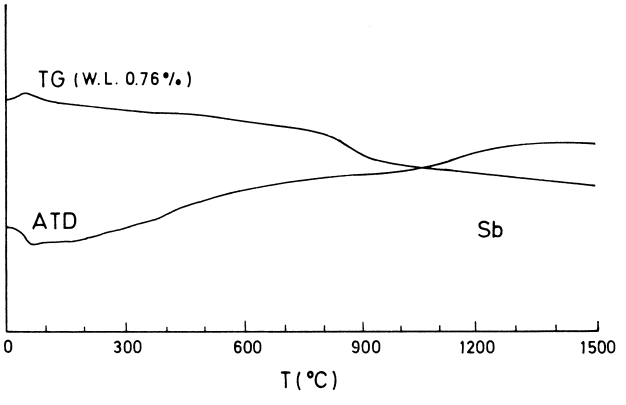

Fig. 3. TGA-DTA curves of beneficiated sillimanite.

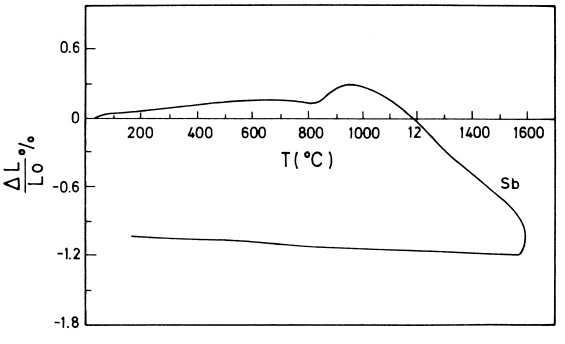

Fig. 4. Dilatometry of beneficiated sillimanite.

temperature of a stable liquid phase from 1587°C, the invariant point in the Al_2O_3–SiO_2 system, to 983°C in the Al_2O_3–SiO_2–K_2O system. The expansion effect associated with the commencement of mullite formation at temperatures ~1450°C, was hidden by the contraction effect produced by the sintering of the sample in the presence of a liquid phase. Another effect attributed to the presence of a liquid phase was the dissolution in the liquid of all silica formed during the transformation reaction of sillimanite aggregates. Consequently cristobalite nucleation and formation did not take place.

Thermal treatments at temperatures higher than 1550°C, very close to the eutectic invariant point in the Al_2O_3–SiO_2 system, produced an important amount of liquid phase, which justified the noticeable increases of the shrinkage rate observed. Again, the expansion effect produced by the sillimanite–mullite transformation was prevented by the contraction effect associated to the sintering process of the sample in presence of liquid phase.

3.3. XRD and FT-IR studies

The thermal transformation of the beneficiated sillimanite material (3 ($Al_2O_3.SiO_2$) —> $3Al_2O_3.2SiO_2 + SiO_2$) was also followed by XRD and FT-IR analyses.

The crystal structures of sillimanite and mullite are closely related, so, their diffraction patterns are very similar [7,8]. However, some characteristic diffractions from both materials can be used to study the thermal transformation of sillimanite. Sillimanite peak diffractions (file 22–18) at 54.5° 2θ and 60.9° 2θ and mullite ones (file 15–776) at 54.1° 2θ and 60.7° 2θ are distinctive for identification. Figs. 5 and 6 show the X-ray diffractograms of samples treated at the different temperatures up to 1650°C and that of the untreated one. The diffraction pattern at 1300°C, does not differ from that of the untreated sample. At 1500°C, the diagram shows weak diffraction peaks corresponding to mullite and broader sillimanite peaks in positions close to those of mullite. The broadened sillimanite reflections it indicate a disordering within sillimanite structure prior to mullitization. By increasing the temperature, the intensities of the last peaks enlarged with simultaneous diminution of the intensities of the sillimanite ones. After treatment at 1600°C, little sillimanite remains while at 1650°C only mullite was identified. Also, a progressive shifts of the doubled peak at 26.2°2θ to lower angles was observed, indicating mullite crystallization. The results of the XRD study are in agreement with those obtained by infrared spectroscopy. FT-IR spectra of the treated samples (1550, 1575 and 1600°C) together with that of the untreated one are shown in Fig. 7. Silica formation is followed by the appearance of two bands at 1104 and 466 cm^{-1}, corresponding respectively to Si-O bond stretching and O-Si-O bond bending

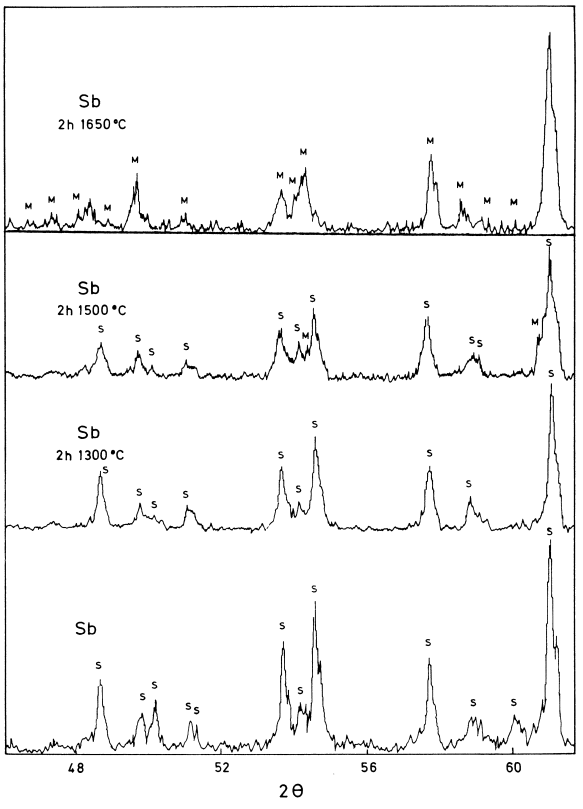

Fig. 5. XRD patterns of the thermal treatments at 1300,1500 and 1650°C/4 h of sillimanite (S_b).

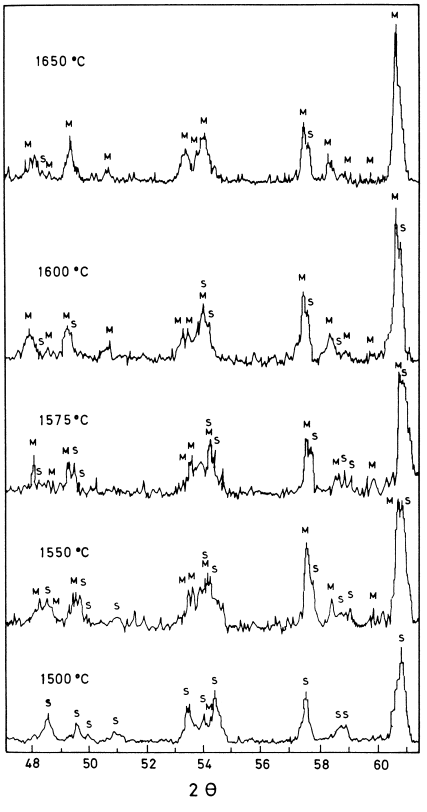

Fig. 6. XRD patterns of the thermal treatments between 1500 and 1650°C/4 h of sillimanite (S_b).

vibrations modes. The presence of the double peak at 1164 and 1137 cm^{-1} (Al-O and Si-O bond stretching vibrations modes) and the band at 537 cm^{-1} (O-Al-O bond bending vibrations mode in AlO_4 tetrahedra) assigned to mullite [9,10] shows the formation of this phase. The intensity of sillimanite bands at 1180 and 950 cm^{-1} (Al-O and Si-O bond stretching vibrations modes) diminishes with the increment of the treatment temperature. At 1600°C, these signals are almost missing.

From the results obtained by XRD and FT-IR, it can be concluded that the larger part of the mullitization of sillimanite takes place between 1550 and 1650°C. A rapid nucleation occurs above a critical temperature, 1550°C, due to the resemblance of sillimanite and mullite structures. Below this temperature, there is a limited transformation in good agreement with previous results [10].

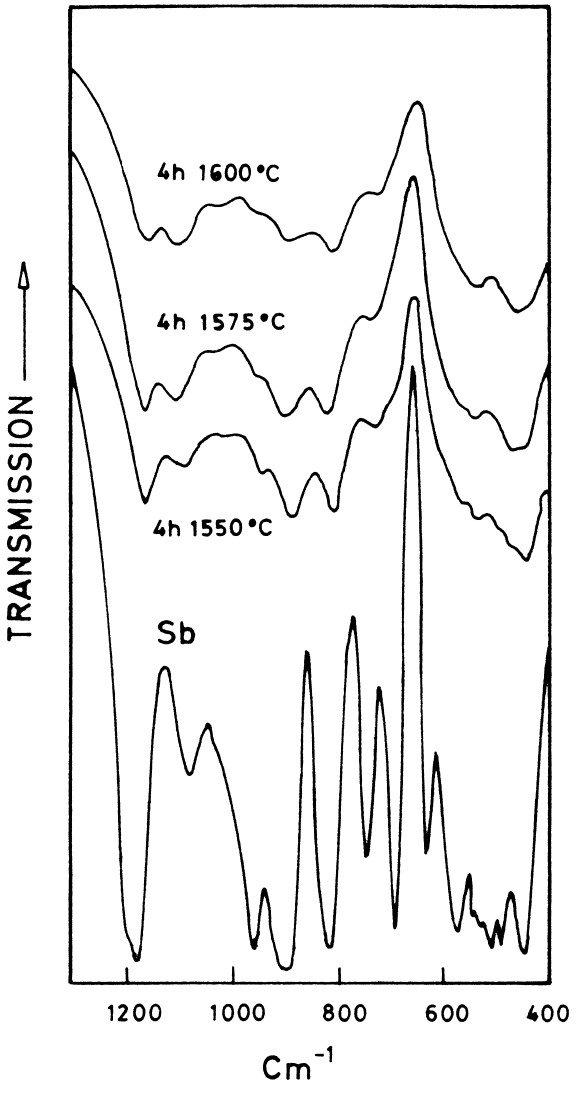

Fig. 7. Infrared transmission curves of sillimanite (S_b) treated between 1500 and 1600°C/4 h.

3.4. SEM-EDS study

Due to the high temperature of mullitization of sillimanite, it is expected that the mullite grain growth takes place almost simultaneously with the nucleation stage. Scanning electron microscopy observations (SEM-EDS) was used to study the transformation. In Fig. 8 (sample treated at 1550°C/4 h), elongated mullite grains and mullite crystals growing on the surface of the partially transformed sillimanite grains were observed. From this figure we found evidence that earlier-formed oriented mullite grows on the surface of the sillimanite grain. The degree of transformation was large which suggest that the transformation process started at temperatures around 1500°C, according to XRD and previously reported results [11].

At temperatures higher than 1550°C (Figs. 9 and 10), a rapid transformation seems to take place throughout the grains which always produces elongated mullite crystals, having a preferred orientation along the direction of elongation of sillimanite crystals. This has been attributed to lower interfacial energies of crystal faces parallel to the "c" axis direction [12], coincident with the elongation direction of the crystals.

In Fig. 11, which correspond to the sample treated at 1600°C/4 h, mullite formation can be observed both perpendicular and parallel to the growing direction (elongation direction of sillimanite). This is related with crystal orientation of the sillimanite aggregates and confirmed that mullite crystals always having a preferred growth direction along the "c" axis of sillimanite. This effect can be observed at high magnification in the Fig. 12. This behaviour is in concordance with the same effect detected by the authors in a previous study [13] on

Fig. 8. Scanning electron micrograph showing needle-like mullite grains growing on the surface of the partially transformed sillimanite (S_b) grains.

the microstructural evolution of mullite during thermal transformation of kyanite.

Finally SiO_2 forms small droplets on the surface of some annealed sillimanite aggregates (Fig. 13). Transformation of sillimanite to mullite and silica produces X-ray amorphous silica (liquid) and not cristobalite as a reaction product. This effect is also a consequence of the alkaline impurities, which formed liquid phase at lower temperature and, as was previously indicated, free silica generated during the transformation goes into the liquid phase. Finally EDS microanalysis carried out in several mullite grains in samples treated between 1550 and 1650°C showed the presence of small amounts of iron oxide in solid solution (Fig. 14). In this case the

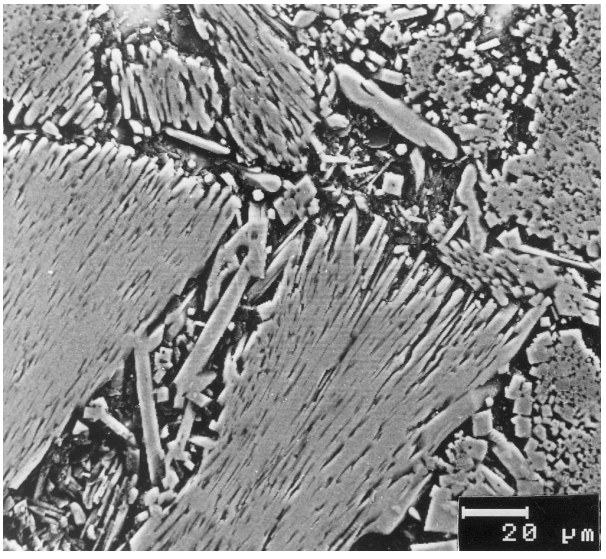

Fig. 9. Scanning electron micrograph showing the total transformation to mullite of sillimanite grains at 1550°C.

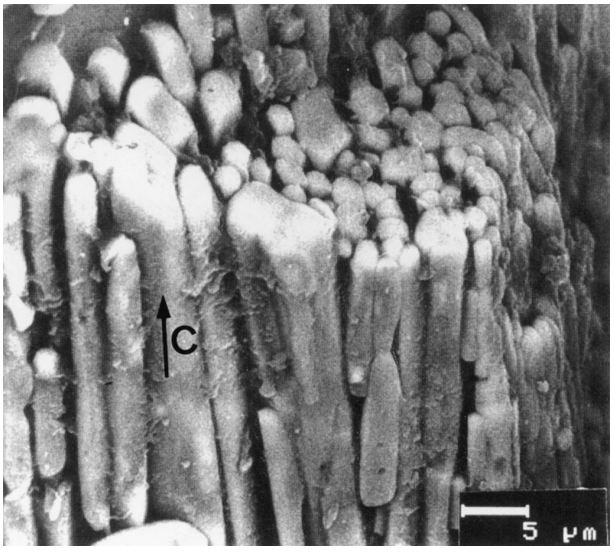

Fig. 10. Scanning electron micrograph of the elongated mullite crystals oriented along the direction of elongation of sillimanite grains.

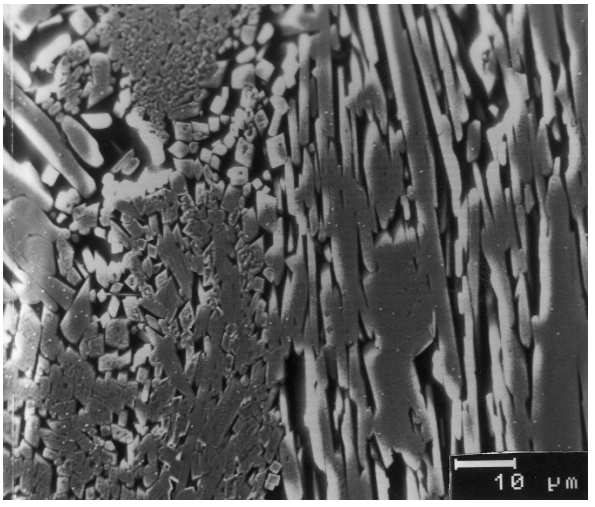

Fig. 11. Scanning electron micrograph showing mullite formation in sillimanite aggregates.

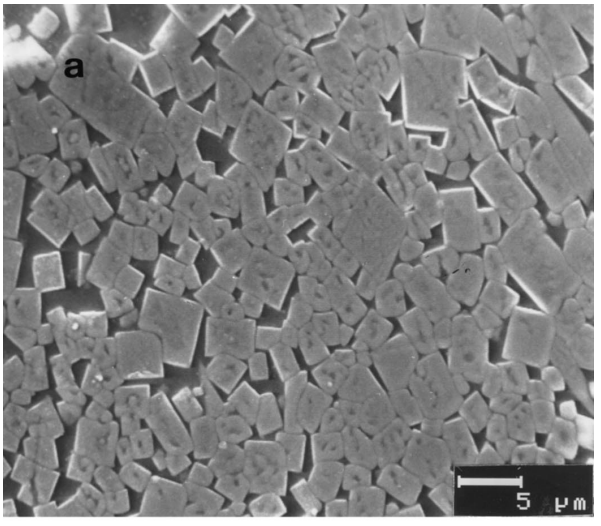

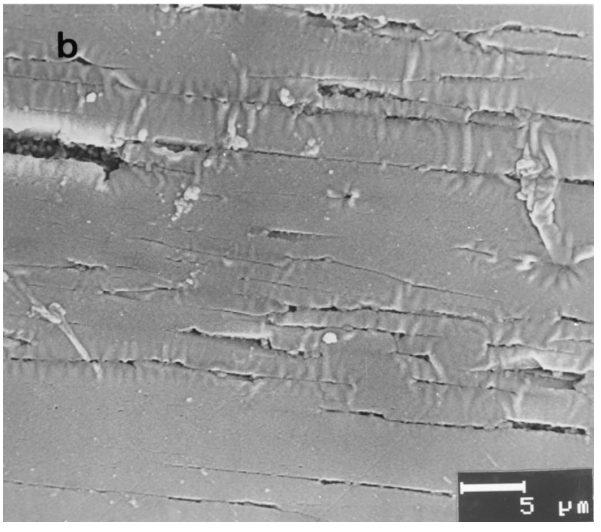

Fig. 12. Scanning electron micrograph of the mullite crystals, perpendicular (a) and parallel (b) to the growing direction.

transformation process was not affected by iron oxide content because of its location in solid solution in mullite structure.

3.5. Leaching purification

From the above analysis, the mullitization conditions selected to obtain a relatively high degree of transformation of sillimanite to mullite, without excessive grain growth, were to heat at 1575°C for 4 h. This material was ground up to obtain a mean particle size of 3 μm. The powder was subjected to HF leaching [14] in order to remove the glassy phase generated during sillimanite-mullite transformation. The leaching conditions used allowed the elimination of silica glass with an efficiency equal to 75 wt%.

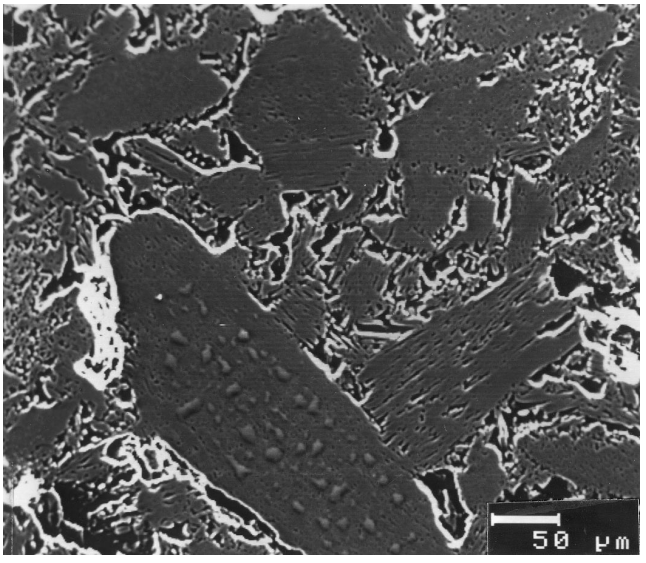

Fig. 13. Scanning electron micrograph of mullite aggregates. It can be seen that SiO_2 form small droplets.

The composition of the leached material was determined by chemical analyses (Table 2). In the same table, the mean particle size and specific surface area are shown. The main impurity of this material was iron oxide (0.45 wt%). It is very difficult to reduce the Fe_2O_3 level below this value because the iron oxide is in solid solution in mullite. The amount of alkaline and earth alkaline oxides were reduced to minimum value. The alumina/silica ratio is very close to the stoichiometric 3:2 mullite.

The specific surface area of the leached material (4.8 m^2/g) is high for non porous solids with a mean particle diameter of 2.7 μm. This value suggests that the leaching processing allowed not only the elimination of the glassy phase but also to partial attack of mullite by HF.

Table 2
Chemical composition of mullite after leaching (wt%)

Mullite obtained	
SiO_2	29.20
Al_2O_3	70.11
Fe_2O_3	0.45
TiO_2	n.d.
CaO	0.09
MgO	0.08
Na_2O	0.04
K_2O	0.03
S_e (m^2/g)	4.8
D_{50} (μm)	2.7

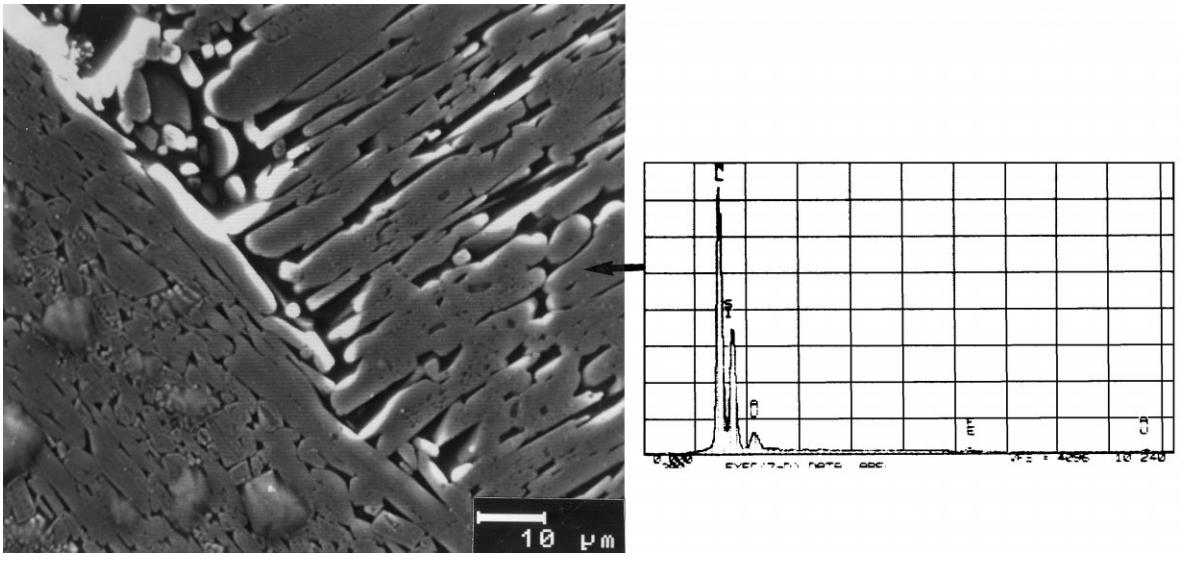

Fig. 14. Scanning electron micrograph and EDS microanalysis of mullite grains showed the presence of iron oxide in solid solution.

4. Conclusions

It can be concluded that the larger part of the mullitization of sillimanite takes place in a temperature interval between 1550 and 1650°C. At these temperatures, the transformation produces liquid and mullite, which is oriented parallel to the elongation direction of the original sillimanite. Elongated mullite grains with a high degree of orientation are always produced.

A rapid nucleation occurs above a critical temperature, 1550°C, due to the resemblance of sillimanite and mullite structures. At this temperature we found evidence that earlier-formed oriented mullite takes place in the surface of the sillimanite grain. Below 1500°C, there is no evidence of sillimanite–mullite transformation.

The critical temperature (1550°C) of sillimanite to mullite transformation was not modified by presence of liquid phase due to the minor impurities in the starting material.

References

[1] H. Schneider, K. Okada, J.A. Pask, Mullite and Mullite Ceramics, John Wiley & Sons, Chichester, 1994.
[2] A. Skillen, Sillimanite minerals. Simplicity the key, Industrial Minerals. Refractories Survey, pp. 57–63, 1993.
[3] D. Gyepesová, S. Durovic, Single-crystal Study of thermal decomposition of sillimanite, Silikáty 2 (1977) 147–149.
[4] M.D. Sacks, H.W. Lee, A review of powder preparation methods and densification procedures for fabricating high density mullite, S. Somiya, R.F. Davis, J.A. Pask (Eds.), Ceramics Transactions, vol.6, Mullite and Mullite Matrix Composites, The Am. Ceram. Soc, Westerville, OH, 1990, pp. 167–207.
[5] I.A. Aksay, D.M Dabbs, M. Sarikaya, Mullite for structural, electronic, and optical applications, J. Am. Ceram. Soc. 74 (1991) 2343–2358.
[6] R.E. Caligaris, A. Vanola, L.A. Zamboni, Actas I Jornadas Argentinas en Ciencia de los Materiales, 1991, pp. 233–236.
[7] W.A. Deer, R.A. Howie, J. Zussman, Sillimanite, Rock Forming Minerals. vol.1A, 2nd ed., Longman Group Limited, 1982, pp. 719–740.
[8] J. Grofcsik, Mullite, Its Structure, Formation and Significance, Academic Kiado, Hungarian Academy of Sciences, Budapest, 1961, pp. 45–60.
[9] H. Schneider, U. Hornemann, Shock-induced transformation of sillimanite powders, J. Mater. Sci. 16 (1981) 45–49.
[10] Ph. Colomban, Structure of oxide gels and glasses by infrared and raman scattering. Part 2, J. Mater. Sci. 24 (1989) 3011–3020.
[11] T. Power, Sillimanite minerals. Europe places demands on andalusite, Industrial Minerals. Refractories Survey, 1986, pp. 77–91.
[12] S.M. Johnson, J.A. Pask, Role of impurities on formation of mullite from kaolinite and Al_2O_3–SiO_2 Mixtures, Am. Ceram. Soc. Bull. 61 (8) (1982) 838–842.
[13] M.A. Sainz, F.J. Serrano, J. Bastida, A. Caballero, Microstructural evolution and growth of crystallite size of mullite during thermal transformation of kyanite, J. Eur. Ceram. Soc. 17 (1997) 1277–1284.
[14] Z. Wancheng, Z. Litong, F. Hengzhi, Modification of the hydrofluoric acid leaching technique: Part I, J. Am. Ceram. Soc. 71 (5) (1988) 395–398.